Proceedings of the 7th Int. Conf. on Hydroscience and Engineering (ICHE-2006),Sep 10 –Sep 13,Philadelphia,USA
ISBN: 0977447405, **Drexel E-Repository and Archive http://idea.library.drexel.edu/**

TIDALLY INDUCED CHANGES OF FLUID PRESSURE, GEOTHERMAL TEMPERATURE AND ROCK SEISMICITY

Hongbing Sun[1], Manfred Koch[2], and Andrew Markoe[3]

ABSTRACT

This paper analyzes and summarizes the numerous types of variations of groundwater pressures (heads), mid-oceanic ridge borehole temperatures and microseismicity in response to tidal forcing in coastal aquifers and deep sea sediments. Tidally related data obtained from various sources were filtered and processed by means of classical harmonic analysis to extract the amplitudes of pressure and temperature fluctuations at different depths, as well as seismicity tilting angles. It is apparent that ocean tidal fluid pressure signals are transported vertically and damp with depth in coastal aquifers and in deep sea sediments. In contrast, the opposite is true for tidal signals triggered by the solid earth tide, as they increase with depth. The vertically transported ocean tidal fluid pressure induces a periodical temperature change in the borehole fluid whose amplitude damps with depth and interrupts the geothermal gradient normally measured in the deep sea sediment. Using the adiabatic state equation of temperature, pressure and salinity (P-S-T), we are able to demonstrate to certain extent that observed periodical temperature changes in the borehole fluid by means of the measured tidally induced fluid pressure changes at the open end of the borehole. A clearly tidal effect was also observed in the filtered seismicity tilting data. Overall, geological phenomena induced by tidal forcing are probably more prominent and complicated than has been realized so far and warrant further investigations. The last section of the paper discusses the analytical prediction of propagation of tidal pressure with depth considering the aquifer deformation. The analytical solution and its application to ODP hole 1025c show that one can predict the vertical pressure change in a well or ODP borehole fairly well with an analytical solution.

Keywords: Tide, groundwater fluctuation, geothermal temperature, seismicity.

Corresponding Author: hsun@rider.edu, 609-896-5185.
[1]Department of Geological, Environmental and Marine Sciences, [3]Department of Mathematics,
[1,3]Rider University, Lawrenceville, New Jersey, USA.
[2]Department of Geohydraulics and Engineering Hydrology,
University of Kassel, Kurt-Wolters Strasse 3, 34109 Kassel, Germany.

1. INTRODUCTION

Ocean tide and solid earth tide are two tidal phenomena produced by the gravitational pull between the earth and the moon and sun. Notwithstanding their common origins, the effects of the ocean and the solid earth tide are very different. Whereas the solid earth tide results in strains or deformations of the rigid earth‘s crust on a global scale (Melchior, 1983), the ocean tide, naturally, is primarily observed only in the open ocean and is felt, as a consequence of the ocean load it induces, in the subsurface of the coastal regions, where it superposes onto the load due to the solid earth tide. The effects of both the solid earth and the ocean tides are felt in aquifer boreholes as fluctuating groundwater levels with, of course, a diminishing contribution of the latter as one moves away from an oceanic coast. On the other hand, since the theoretical strains induced by the solid tidal potential are about two orders of magnitude smaller than those due to the oceanic tidal load (Melchior, 1983; Rojstaczer and Agnew, 1989), it is generally not an easy task to distinguish both contributions at locations away from the open ocean (Tolstoy et al., 2002).

Beginning with the pioneering studies of Melchior in the 1960's (see Melchior, 1983 and references herein) many studies, at the interface of hydrology and geophysics, have been undertaken since then to investigate the effects of, namely, solid earth tides, onto aquifer systems and to either determine hydraulic and poroelastic aquifer properties or to quantify the tidal signals from their aquifer responses (e.g. Bredehoeft, 1967; Marine, 1975; Van der Kamp and Gale, 1983; Hsieh et al., 1987, Sun, 1997, Zaske et al., 2000; Jupp, 2000).

For the ocean seafloor, comparing the generating tidal signals and the well responses in various mid-ocean ridge hydrothermal systems, numerous studies (Little et al., 1998, Davis et al, 1995, 2000, Johnson and Tunnicliffe, 1985; Schultz, 1992; Wetzler et al., 1998, Davis and Becker, 1994, 1999, Jupp, 2000) have clearly pointed out the strong influence of the local ocean tidal load onto the fluid- and thermodynamic behaviour of the convecting flow circulation. Moreover, as the solid earth tidal signal may reach loading peaks of up to 2 kPa/hr, superimposing on a tectonic loading rate of around 0.1 kPa/hr, it has been argued that they may trigger earthquakes, i.e. have an impact on the seismicity, particularly in the vicinity of mid-oceanic volcanoes where there is an additional amplification due to the ocean tidal load (e.g. Rydelek et al., 1988; Tolstoy et al., 2002).

From a physics point of view, and as will also be laid out mathematically in the theoretical section, the vertical propagation of a tidal signal will depend on both the characteristics of the tidal source and of the conducting media. Mechanically, the signal from the oceanic load represents a pressure force on the earth‘s surface (ocean bottom) that penetrates diffusively in vertical and horizontal directions (Van der Kamp and Gale, 1983). This means that, as the load tidal signal propagates away from the open water into the groundwater or into a borehole fluid, the strength of the signal will decrease asymptotically. On the contrary, the solid earth tide signal acts as a volume (pressure) force for dilatation over the total extent of the solid body (aquifer). The related pressure pulse of water is theoretically invariant of depth given the same porosity, although it changes, because of the earth‘s rotation and of varying sun and moon constellations, with the earth coordinate of the observation point. One section of the present paper will present a comparison of two types of tide for the purpose of illustrating their differences such that one can determine the primary tide that contributes to the pressure, temperature and seismicity change in the well and the borehole fluid. In

addition, an attempt will be made to qualitatively illustrate the point that the geothermal temperature change in borehole fluid in response to the tidal pressure is a result of the complicated pressure-temperature-salinity interaction due to equilibrium requirement of the state of water. That objective is to clarify some of the current confusing explanations that prevail on this subject. To this avail we will study the changes of propagation of tidal signals in a vertical direction through sediments, for both land wells and ODP drill holes.

2. TIDALLY INDUCED PHENOMENA

2.1. Ocean tidally induced groundwater level changes as a function of depth

As mentioned in the introduction, in a coastal region one can clearly assume that fluctuations of the

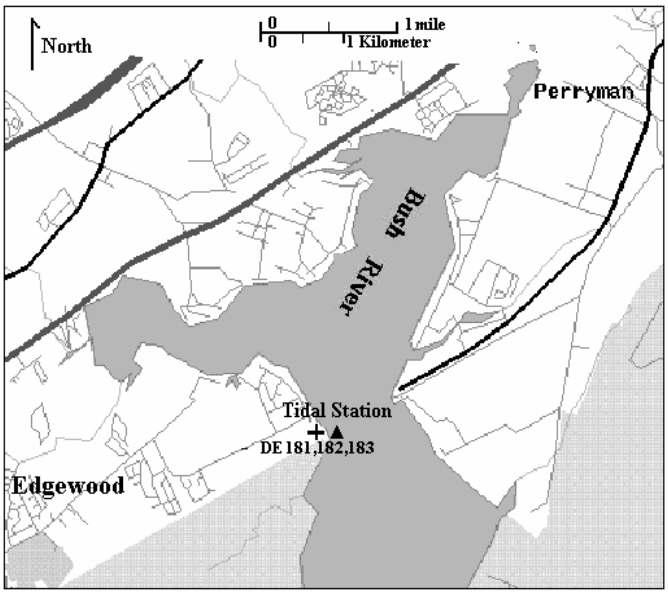

Figure 1. Location map of the cluster wells HA De 181,182,183 and tidal station in Bush River, a tributary of Chesapeake Bay in Maryland

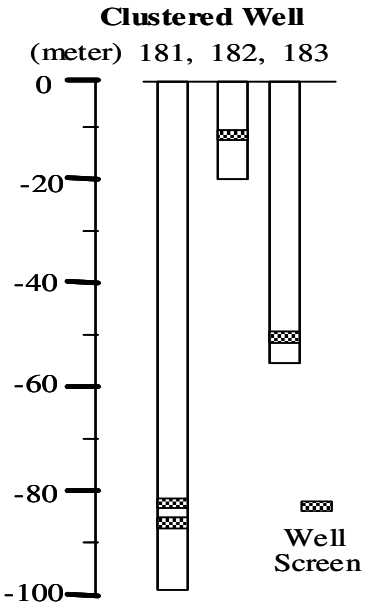

Figure 2. Sketched cross-section of the clustered wells along one of the tributary of Chesapeake Bay, Maryland.

hydraulic pressure or head are much more influenced by the ocean tide than by the solid earth tide. To test this hypothesis further we first investigate water level data of three clustered wells along the tidally influenced Bush River, which is a tributary of the Chesapeake Bay near Edgewood in Maryland (Figure 1). The three wells are about 73 meters away from the river bank (Drummond and Blomquist, 1993) and tap the Talbot Formation aquifer that consists of a sediment mixture of clay, silt, sand and gravel, at screening depths of 10.7m, 48.8m and 83.9m (Figure 2). Three series of water level data taken at 60-minutes intervals from July 1988 to July 1989 were obtained from the US Geological Survey and the tidal elevations from the Maryland Geological Survey. Because the raw data are relatively rough, they are further processed such that the high frequency noise was removed by the moving average filtering method as described by Hsieh et al. (1987). Figure 3

presents traces of the tidal gage heights and of the smoothed water fluctuations from the three clustered wells where, for illustrative purposes, only a time span of one week is shown. Firstly one observes the clear correlation of the groundwater heads in all three wells with the tidal elevations and, secondly, the decreasing amplitudes of the head variations with the screening depth of the wells.

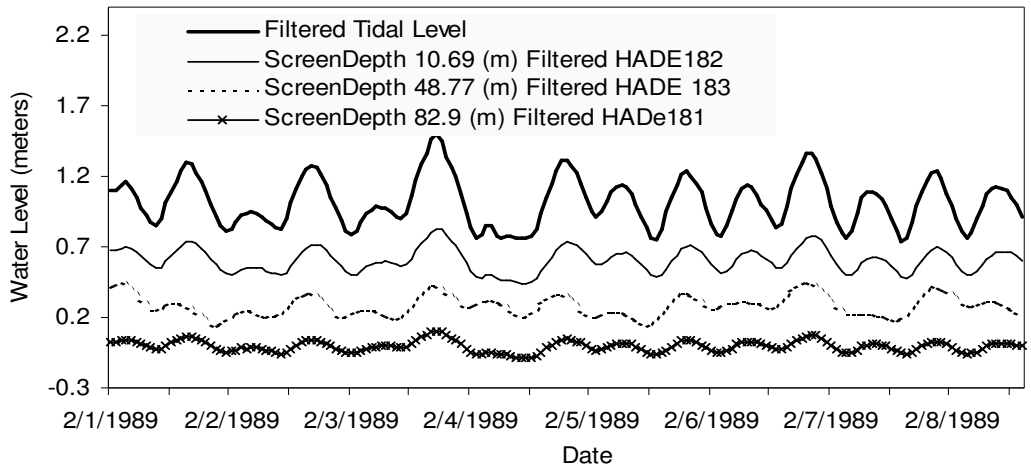

Figure 3. Upper panel: Time series of tidal variations (upper trace) and of the groundwater level fluctuations for the three wells from February 1 to 9 of 1989. The legends indicate the screen depth of the clustered wells. Right panel: Plot of semi-diurnal ($M_2 + S_2$) and diurnal ($K_1 + O_1$) amplitudes versus well screen depth. Diurnal tide has a 24-hour period and semi-diurnal tide has a 12-hour period.

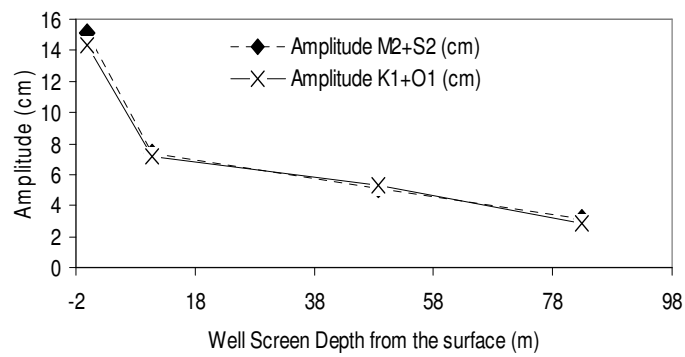

A more quantitative analysis of this trend is derived from the least square harmonic analyses of the filtered tidal groundwater levels. Because more than 29 days of water level data were available we could use Boon and Kiley's (1978) least square harmonic analysis program to compute the major diurnal ($K_1 + O_1$) which has a 24 hour period and semidurnal ($M_2 + S_2$) tidal amplitudes (cf. Sun and Koch, 1998, for further details) (Table 1). These are plotted in Figure 3 as a function of the depth of the wells. This plot clearly indicates how the amplitudes of the groundwater head fluctuations are dampened with depth. As outlined in the introduction, this vertical damping is a consequence of the dissipation that the surficially acting tidal signals undergo as they penetrate into the subsurface. The fluctuations of the hydraulic head in the wells can be predicted by means of a theoretical formula that will be developed in a later section.

2.2 Tidal signals in ODP borehole pressures as a function of depth

Mainly as a result of the activities of the ODP (Ocean Drill Program), tidally modulated signals in

Table 1. Tidal Amplitudes of Tidal Station and Wells

			TidalLevel	HADe182	HADe183	HADe181
			0(m)	15.24(m)	53.34(m)	88.39(m)
			Feb-89	Feb-89	Feb-89	Feb-89
NOS NO.	CONS	T. SPEED	Ampl (cm)	Ampl (cm)	Ampl (cm)	Ampl (cm)
1	M2	28.9841	13.43	6.5	4.66	2.975
2	S2	30	1.729	0.826	0.444	0.171
3	N2	28.4397	2.515	1.595	1.097	0.749
4	K1	15.0411	7.87	3.941	2.743	1.558
5	M4	57.9682	0.884	0.424	0.385	0.292
6	O1	13.943	6.485	3.192	2.588	1.257
7	M6	86.9523	0.276	0.173	0.164	0.099
9	S4	60	0.616	0.044	0.08	0.067
12	S6	90	0.182	0.037	0.085	0.039
36	M8	115.9364	0.186	0.058	0.021	0.012
11	NU2	28.5126	0.51	0.247	0.177	0.113
13	MU2	27.9682	0.322	0.156	0.112	0.071
14	2N2	27.8954	0.349	0.169	0.121	0.077
15	OO1	16.1391	0.279	0.137	0.111	0.054
16	LAM2	29.4556	0.094	0.045	0.033	0.021
18	M1	14.4967	0.46	0.227	0.184	0.089
19	J1	15.5854	0.512	0.252	0.204	0.099
25	RHO1	13.4715	0.246	0.121	0.098	0.048
26	Q1	13.3987	1.258	0.619	0.502	0.244
27	T2	29.9589	0.102	0.049	0.026	0.01
28	R2	30.0411	0.014	0.007	0.004	0.001
29	2Q1	12.8543	0.169	0.083	0.067	0.033
30	P1	14.9589	2.605	1.305	0.908	0.516
33	L2	29.5285	0.376	0.182	0.13	0.083
35	K2	30.0821	0.47	0.225	0.121	0.046

fluid pressures in seafloor boreholes and their possible consequences on various hydrothermal activities have been observed for some time (e.g. Davis and Becker, 1994, Davis et al., 2001, Wang and Davis, 1996, Fujioka et al., 1997, Wang et al., 1999, Jupp, 2000). Long term borehole pressure data for the ODP holes 1025C, 1027C, 1026B, and 857D can be found, for example, in the proceedings of the ODP activity in the Juan De Fuca Ridge area (Davis and Becker, 1994, Davis et al., 1995). Our raw data from these four ODP wells was complemented by pressure data from the PMEL PR site of the Pacific Environmental Laboratory‘s cruise’s (see Figure 4 for locations) and was taken from Davis and Becker (1999). A cross-section of the ODP hole 1027C showing the positions of the pressure transducers and the thermistors is illustrated in Figure 5.

To remove noise and trends, the hourly time series data was either filtered by a 24-hour moving average, or in the presence of stronger noise, by using Hsieh et al.‘s (1987) method, as discussed in the previous section. As can be recognized from the design of the borehole in Figure 5, the fluid pressure measured by the transducer actually represents the pressure exerted by the ocean

load at the vertical position of the open hole at the bottom of the picture. The depth numbers indicated by the legends associated with each data series represent the depth of open hole of the borehole (Figure 5). Similar to Figure 3, the pressure variations were then converted to corresponding water level changes (in centimeters) and, for plotting purposes only, computed as

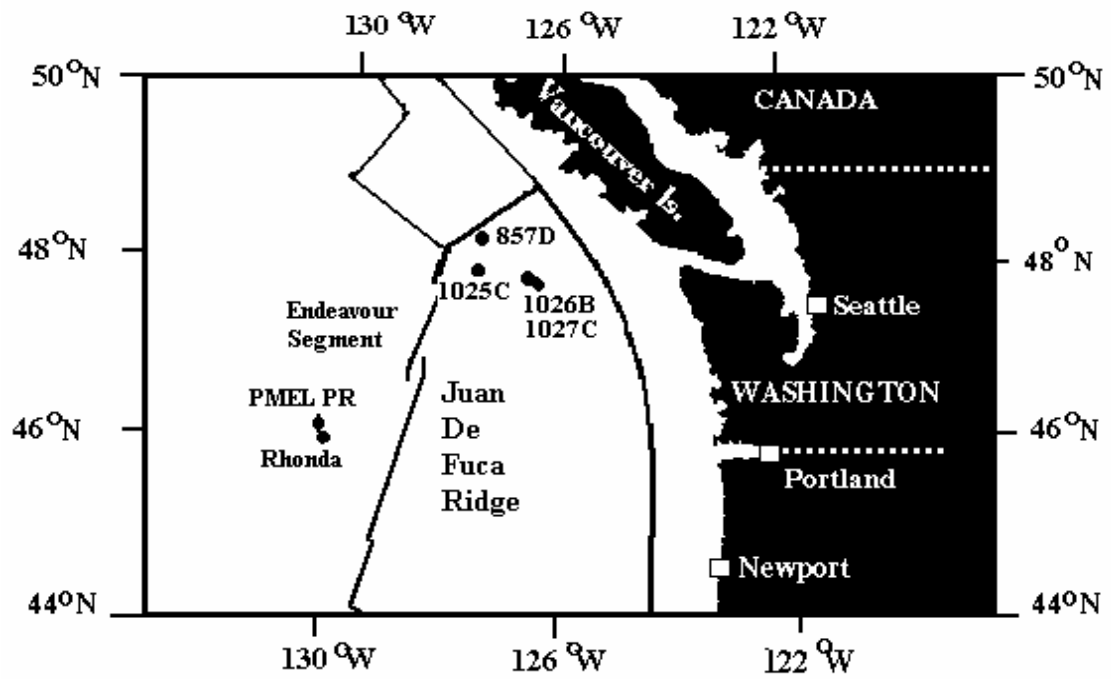

differential values. Figure 6a shows the ---for plotting purposes---arbitrarily shifted hourly-sampled, smoothed fluid pressure time series data of the tidal records at the sea floor and of the three boreholes, whereas the fourth data series from borehole 1027C, which comprises also temperature data, is plotted in Figure 7.

Figure 4. Approximative locations of the ODP wells and the seismicity recorder (Rhonda) in the vicinity of Juan De Fuca Ridge.

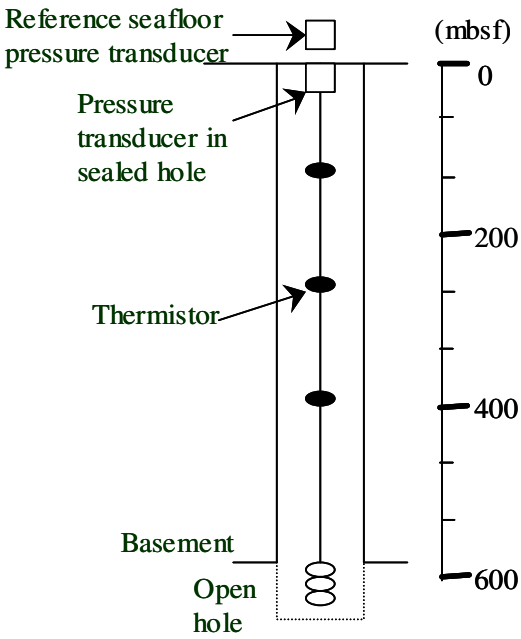

Figure 5. Right picture showing the cross-section of the ODP hole 1027C showing the positions of the pressure transducers and the thermistors.

Again, one notes from Figure 6(Upper panel) a consistent attenuation of the converted

borehole pressure variations with increasing depth of the borehole, i.e. the propagation of the tidally induced pore pressure variations into the subseafloor formation is strongly dampened. This has also been recognized in the theoretical analysis of Wang and Davis (1996). Additionally, comparing the absolute ODP borehole pressure variations with the previously analyzed aquifer hydraulic head data of Figure 3, one observes that the absolute magnitudes of the variations are similar.

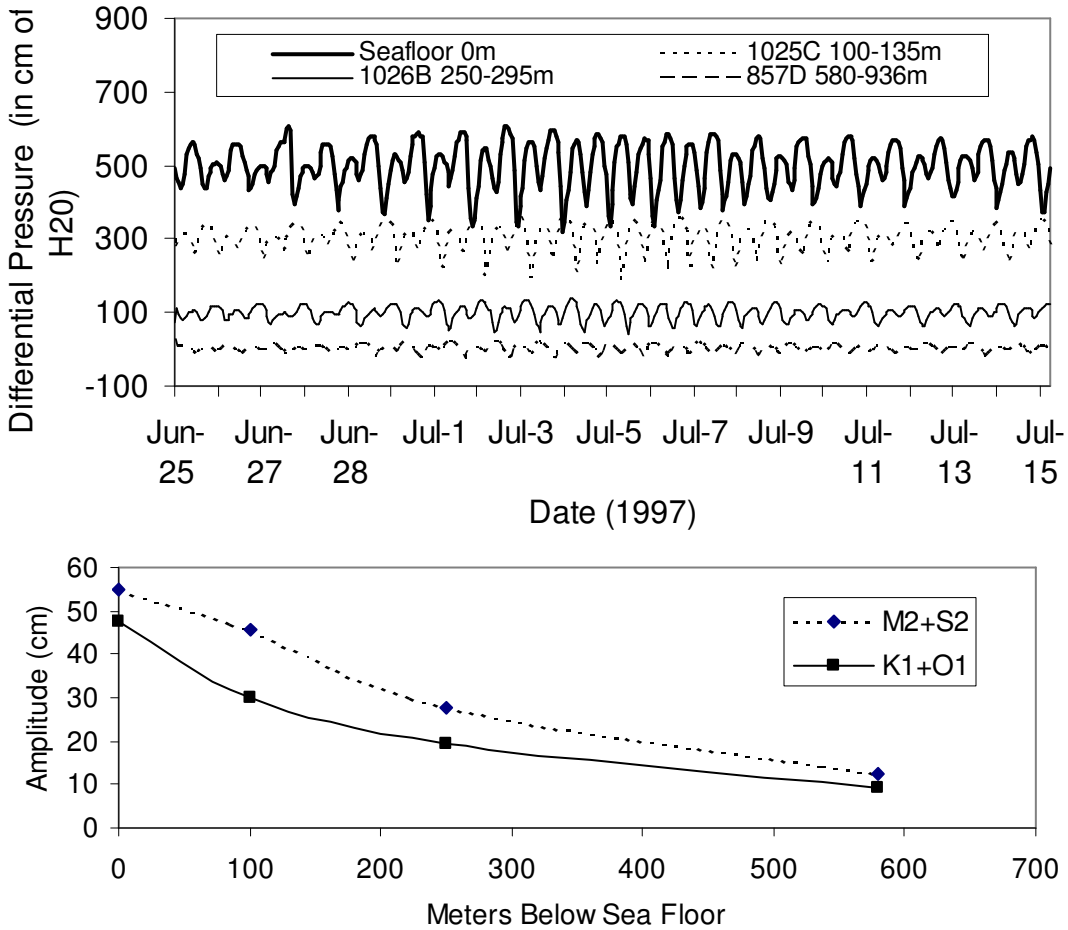

Figure 6. Upper panel: Filtered time series of the pressure variations in cm of H2O for the three ODP holes (original data are from Davis and Becker, 1999). The legend number range for each of the three borehole indicate the screened borehole depth intervall where the pressure is actually measured. Lower Panel: Plot of semi-diurnal ($M_2 + S_2$) and diurnal amplitudes ($K_1 + O_1$) versus open hole depth.

For further quantification of this damping behavior, the amplitudes of the major harmonic components were calculated. Because the tidal data record we obtained from Davis and Becker was shorter than 29 days, we resort to use Foreman's harmonic analysis program (Foreman, 1979), instead of that of Boon and Kiley (1978) used previously, since the former can handle less than 29 days of hourly water level data. Although Foreman's method yields a smaller number of harmonic components, it is sufficient for the purpose of the present analysis. Harmonic analysis for data less

than 29 days was also discussed by Jupp (2000), who favored the British Admiralty Method in such a situation.

The application of the Foreman's harmonic analysis to the three-week-long pressure data record results in the semi-diurnal ($M_2 + S_2$) and diurnal ($K_1 + O_1$) tide amplitudes shown in Figure 6 (Lower panel). One notes again the clear exponential damping with increasing depth of the borehole. Moreover, similar to the cases of horizontal damping of tidal waves in a coastal aquifer (Sun and Koch, 1998) and of the damping of tidal waves in an open esturary (Sun and Koch, 1999) one would expect the high frequency, semidurnal tidal signal to damp faster than the low frequency, diurnal tidal signal, due to the skin-effect. However, this appears to be neither the case for the ODP boreholes in Figure 6 nor for the aquifer wells in Figure 3. As done in Sun and Koch (1998), the analysis of the damping speeds allows one to obtain the storativity/transmissivity ratio of the aquifer and/or of the sediments. If the storativity is considered insensitive to the water level fluctuations, as suggested by Hsieh et al. (1987), then the rate of the amplitude damping essentially reflects the transmissivity of the sediments. We will discuss the reasons for this departure of the data behavior from the theoretical predictions in a later section. Finally, from Figure 6 (Upper panel) one notices also a time lag when the tidal signal propagates downwards.

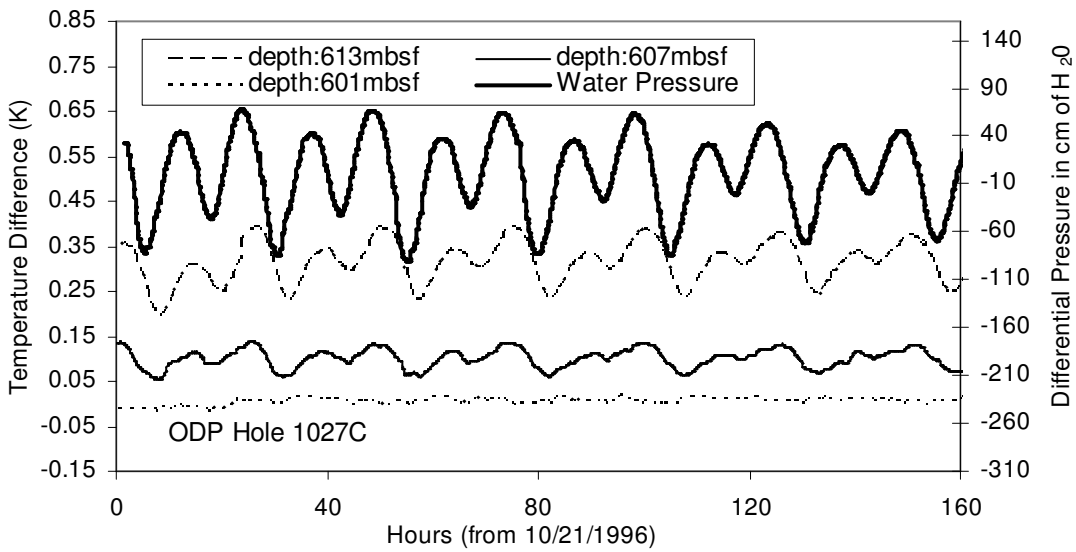

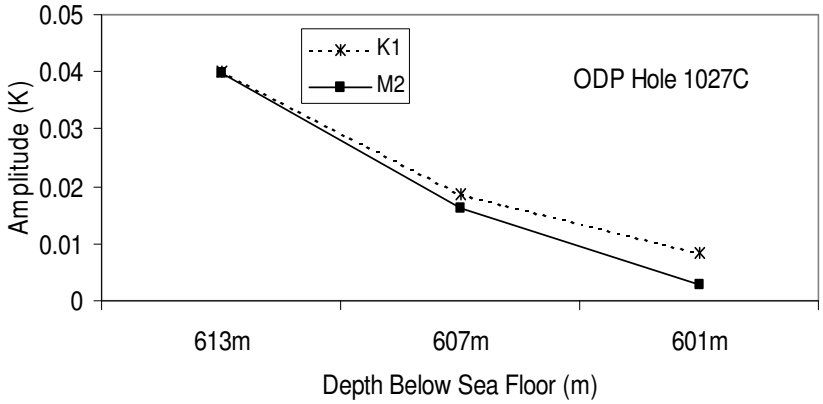

Figure 7. Upper panel: Time series of temperature fluctuations at various depths in the open borehole vs. differential pressure of water at the sea floor. Right panel: Plot of amplitudes vs depth positions of thermistors (Original data are from Davis and Becker, 1999).

2.3 Tidal signals in borehole fluid temperatures as a function of depth

Tidally modulated geothermal temperatures in ODP borehole fluids provide rich information on various aspects of hydrothermal activities underneath the seafloor (e.g. Jupp, 2000). The Endeavour segment and the Pipe Organ vent of Juan de Fuca Ridge (Johnson and Tunnicliffe, 1985; Schultz, 1992; Wetzler et al., 1998), the Middle Valley time series geothermal data in ODP holes 857D and 858G (Davis and Becker, 1999), Cascadian Accretionary Prism (Davis et al., 1995, Nova Vent Program, 2002 at www.nova.gov), the Guaymas Basin of Gulf of California (Little et al., 1988), Rose Garden site of East Pacific Rise and southern East Pacific Rise (Jupp, 2000) were all reported to be locations exhibiting strong effects of ocean tidal signals on geothermal temperatures.

To further investigate how tidally affected geothermal temperatures change with the depth of the deep ocean sediment, we use a two-week-long record of the ODP hole 1027C temperature data published by Davis and Becker (1999), which is shown, after the usual filtering process, in Figure 7a. One observes that the temperature fluctuations go in tandem with the fluid pressure fluctuations, though there is phase shift between the two that becomes larger with increasing depth. Employing again Foreman's harmonic analysis program (1979) the amplitude plot of the temperature variations for the semi-diurnal and diurnal components shown in Figure 7b manifests quantitatively the change of the temperature fluctuations with depth, namely, that they are now increasing.

The first question that arises from Figure 7(Upper panel) is why the fluid temperature varies in response to the tidal fluid pressure? A few explanations have been proposed in the literature. One given by Davis and Becker (1994) is that the ocean tide acts as a hydraulic pump. They used a general tidal pumping concept to explain the coincidence between the high tide and high temperature in the borehole. Anderson et al. (1997) proposed that tidal currents may affect geothermal temperature by moving water of different temperatures back and forth from a fixed spot (Anderson et al., 1997). There is also the theory of thermal diffusion of the variations in bottom water temperature down through the sediment by Kinoshita et al. (1998).

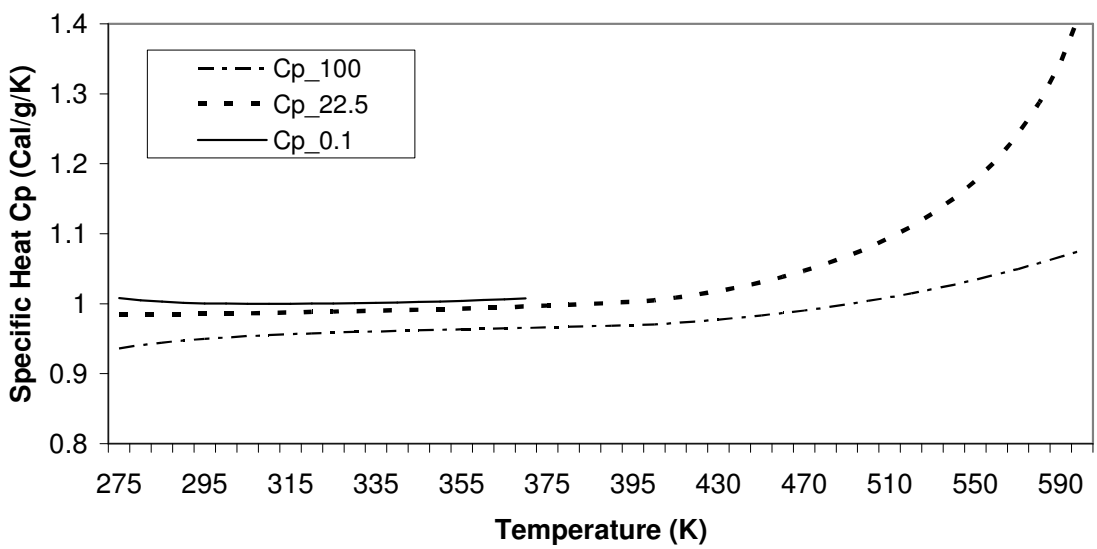

Figure 8. Changes of specific heat coefficient of liquid phase fresh water vs. temperature and pressure change. Data are calculated from thermodynamic equation of Wagner and Pruβ (2002). Where 0.1, 22.5 and

100 in the legend denote the pressure levels in MPa at which the corresponding coefficient curve was. 0.1 is close to one atmosphere and 22.5 MPa is close to the water pressure at the seafloor in the vicinity of Juan De Fuca Ridge.

Though the exact mechanism still needs to be worked out, it is generally agreed that the vertical fluid motion induced by tidal fluctuation in the borehore plays a significant role on the temperature fluctuation of the thermal fluid. In addition, we thought initially that the change of state of thermal fluid based on the thermodynamic relationship of pressure, temperature and salinity (P-T-S) in response to pressure change may also be important in a thermal fluid situation. This potential temperature change due to pressure variation was examined with the state of the thermal saline fluid equation extracted from the experimental data of Wagner and Pruß(2002), EOS 80 of Millero et al. (1981), and the entropy data of Feistel (2003). The comparison of the temperature change predicted based on the state of the thermal saline fluid with the actual temperature change is given in Table 2 which is insignificant in this particular case. The salinity is based on the chlorine data provided in the ODP leg 168 preliminary report (Shipboard Scientific Party, 1997). The pressure range difference is deduced from the water depth at high and low tides of well 1027C. However, the change of temperature in response to pressure change should more significant as the temperature increases because of the decrease in fluid's specific heat (Figure 8).

Table 2. ODP1027C Temperature Prediction and Coefficients Used

Items	Low	High	Average
Salinity range (psu):	34.90305	36.18280	35.54292
Temperature range(T, C):	58.80000	58.99850	58.89925
Density range (g/cm^3)	1.021690	1.021694	1.01842
Pressure range(P, kPa)	27025.0	27035.0	27030.0
Measured pressure difference:	0.09870 atmosphere		
Measured temperature difference:	0.198500 °C		
Predicted average temperature difference based on the state of the thermal saline fluid equation		0.00046 °C	

The second question arises from Figure 7 (Upper panel) is how the fluctuations of the tidal temperature in the borehole fluid change with depth. As shown in the cross-section of the ODP borehole in Figure 5, the tidally influenced differential pressure measured by the transducer is the tidal differential pressure at the depth of the open hole because the borehole is sealed at its top end. Thus, theoretically, the actual water pressure should decrease upward in an insulated sealed borehole. However, the three data series of Figure 7a are all within the interval of an open hole and this interval crossed two igneous horizons and a sediment layer with quite different thermal conductivities, one could not deduce a conclusive relationship of borehole fluid temperature versus depth based on those data series. However, from the apparent positive correlation of the amplitudes of the sinusoid tide and temperature fluctuations reported (Jupp, 2000), it is reasonable to assume

that as the fluctuations of fluid pressure decrease with depth, so do the fluctuations of temperature in an undisturbed situation. This fluctuation of temperature decreases with depth is also indicated by the measurement from a series of thermistors placed at various depths of the ODP hole 858G by Davis and Becker (1994) and stated explicitly by Wang and Davis (1996).

2.4 Earth tidally induced groundwater level changes as a function of depth

As mentioned in the introduction, effects of the ocean and the solid earth tide are very different. Whereas the solid earth tide results in strains or deformations of the rigid earth's crust on a global scale of the order of $O(10^{-8})$ (Melchior, 1983), the ocean tide acts mainly only in the open ocean and its load induces strains of $O(10^{-6})$ mainly in the subsurface of the coastal regions, where it superposes onto the strains due to the solid earth tide.

Though there may be some practical difficulty in separating the tidal effects of earth tide and ocean tide in the ocean floor, recognition of the effects of the earth tide on groundwater on land is generally not difficult. If the groundwater well is far from the ocean coast and the water levels show tidal periodicities, it can only be from the earth tide. In contrast to the damping of the ocean tidal signals with depth as discussed in Section 2.1, the magnitudes of the hydraulic head fluctuations due to the earth tide should increase with depth (personal communication with Hsieh and Ducarme, May 2002). Bredehoeft (1967) showed that for both confined and unconfined aquifer the amplitudes of the earth tide-induced water level fluctuations are inversely proportional to the porosity. In general, due to the compressibility of the aquifer skeleton and increasing lithostatic overburden, the porosity of geologic deposits decreases with depth, and the amplitudes of the tidal fluctuations should therefore increase. The permeabilities of the confining layers also generally decrease with depth, so that deeper aquifers more closely approximate ideal artesian conditions. This, too, would produce larger earth tidally induced head fluctuations in deeper wells.

In fact, this can be seen in the analysis of water levels of three wells of different depths in South Carolina. The raw data used here is taken from Marine (1975). It was filtered with a 24-hour moving average window twice to remove the high frequency noises and trends. Plots for both the raw data and the amplitudes obtained with Foreman's harmonic analysis show that, in contrast to the damping trends of the ocean tidal signals observed in Section 2.1, the amplitudes of the earth tidal fluctuations of the hydraulic heads increases with depth (Fig. 9).

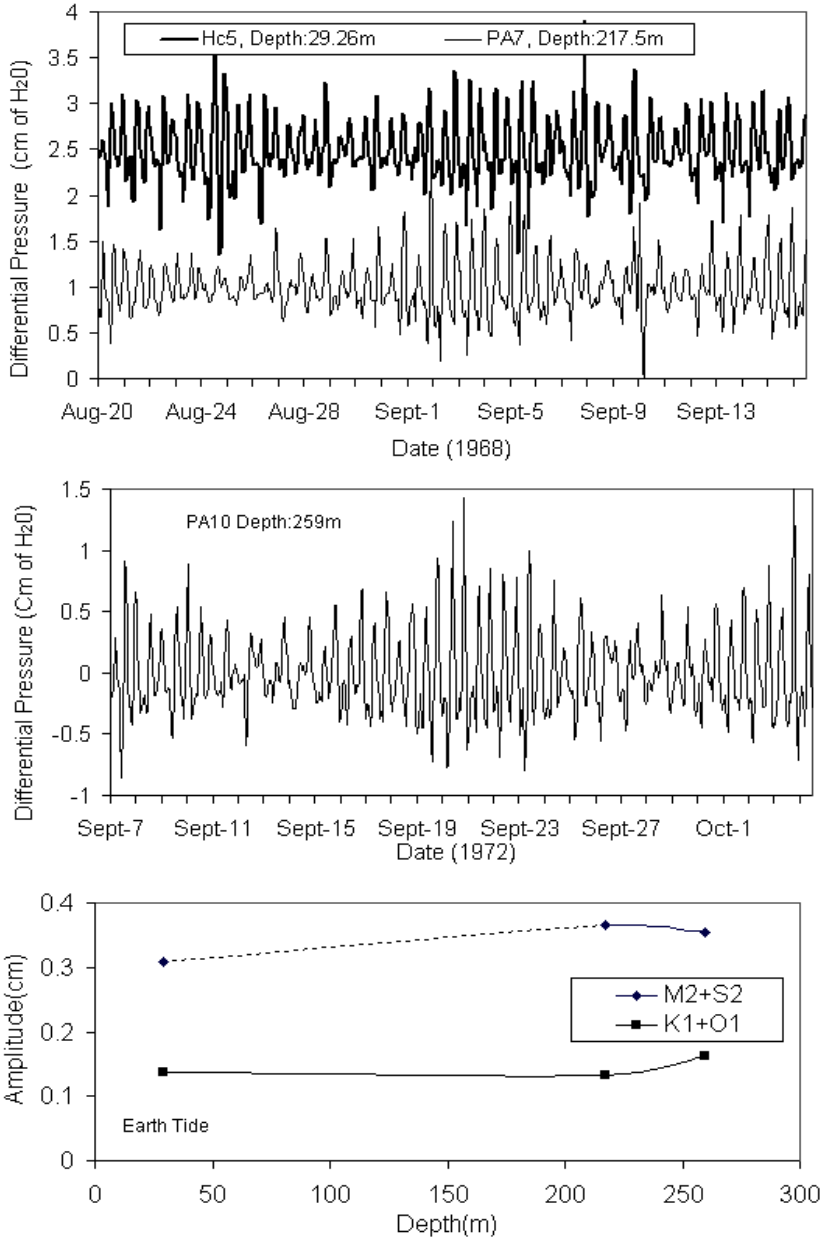

Figure 9. Upper and middle panels: Earth tide related fluctuations of differential pressure time series vs. well depth. Lower Panel: Plot of semi-diurnal (M2+S2) and diurnal amplitudes vs well depth (Data from Marine, 1975).

2.5 Tidally triggered seismicity

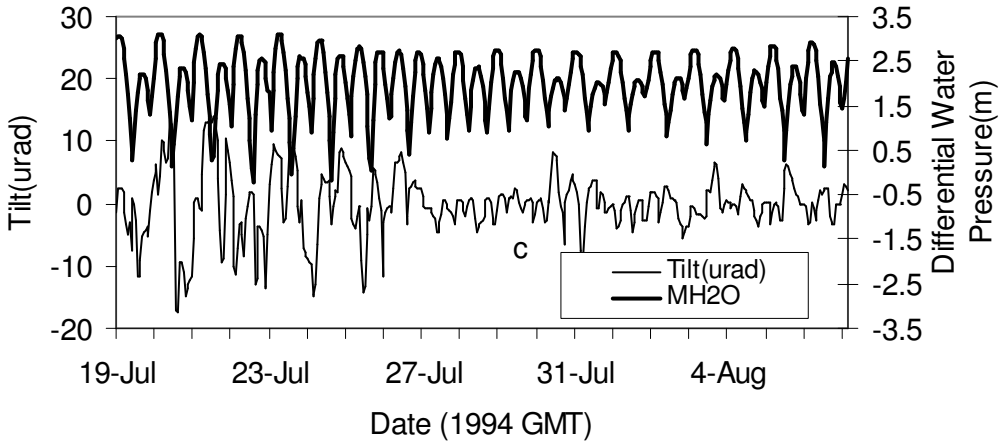

Figure 10. The time series of seafloor differential water pressure and tilt (seismicity) plot (Data are from Anderson et al., 1997).

Effects of tidal signals on the frequency of the earthquakes in the geothermal vents are being reported by many researchers (Rydelek et al., 1988, Tolstoy et al., 2002, Wilcock, 2001). Wilcock (2001) showed that the highest earthquake activity in the Juan de Fuca Ridge occurs when the tidal amplitudes are at a minimum. Since the earthquakes there are mostly of a normal faulting type, the explanation is that extensional stresses are higher in all directions during the low tide. Also, during the low tide, the decrease in the pore pressure might lead to an increase in the effective stress and, therefore, to an increase of the likelihood of fault slippage (Tolstoy et al., 2002). Plot of the data from Juan de Fuca Ridge (Anderson et al., 1997) from the tiltmeter of bore pressure vs. tilt clearly shows they are correlated with the tidal signals (Figure 10, Table 3). And the high tilt value is corresponding to the low tide. We assume the influence of tidal wave on the seismicity frequency decreases with depth as the strength of the tidal signal decreases.

Table 3, Amplitudes of temperature tilt angle and pressure. (1994, Late July to August)

NOS No	Tilt(urad)	Pressure H_2O(cm)
M2	0.6246	74.194
S2	0.7841	13.538
O1	1.0395	26.471
K1	0.6331	36.553

3. PREDICTION OF VERTICAL TIDAL PROPAGATION

3.1. Theory

Potential deformations of the aquifer related with the tidal propagation have been discussed and added in as a source term in the governing equation by various authors (Bear, 1972, Van Der Camp, 1983, Rojstaczer and Riley, 1990, Wang and Davis, 1996). Though, the parameters regarding the consolidation of the aquifer are treated differently, the governing equation of the vertical flow is

generally agreed in publications.

Assuming a homogenous aquifer, following Van Der Camp and Gale (1983)'s approach, the one dimensional vertical flow governing equation is:

$$\frac{\partial^2 p}{\partial z^2} = \frac{S_s}{K}\left(\frac{\partial p}{\partial t} + \gamma\frac{\partial \delta}{\partial t} + 2G\gamma\frac{\partial \varepsilon}{\partial t}\right) \qquad (2)$$

where p is the water pressure and has a unit of meters of water (m), z is the depth of borehole/well from the sea/river bed in meters, S_s is the specific storage in unit of m^{-1}, K is the conductivity with a unit of m/s, ε is the dimensionless horizontal area dilation due to earth tide, G is the rigidity modulus that has a pressure unit, δ is the tidal loading stress that has a pressure unit as well, γ is the dimensionless "tidal loading efficiency" defined by Van Der Camp and Gale, (1983) as:

$$\gamma = \frac{(1+v)}{3(1-v) - 2\alpha\beta(1-2v)}\beta \qquad (3)$$

where α is the coefficient of stress and β is the Skemton ratio and ν is the Poisson's ratio. They are dimensionless.

The differential tidal loading boundary condition at the sea/river floor is:

$$p(z=0,t) = \sum_{k=1}^{n} A_k \cos(a_k t + c_k) = \delta(t) \qquad (4)$$

where A_i is the amplitude of ith tidal constituent in meters of water, a_i is the tidal speed (has a unit of s^{-1}), c_i is the local phase shift term, subscript i indicates the ith tidal constituent and t is time in second.

Following the approaches of Wang and Davis (1996) and Jupp (2000), ignoring the earth tidal component, the analytical solution to (2) is:

$$p(z,t) = p_{z0} + (1-\gamma)\sum_{k=1}^{n} A_k e^{-\sqrt{\frac{S_s}{2K}}z} \cos\left(a_k t - \sqrt{\frac{aS_s}{2K}}z + c_k\right) + \gamma\sum_{n}^{k=1} A_k a_k \cos(a_k t + c_k) \qquad (6)$$

where p_{z0} is the static pressure at depth z.

For tidal predictions at inland wells off the coastline with the boundary condition of (3), it is more appropriate to work with a two dimensional (x-z)-version of the groundwater solution following Carslaw and Jaeger (1959)'s work on heat conduction with a point periodical source.

3.2. Discussion and Application

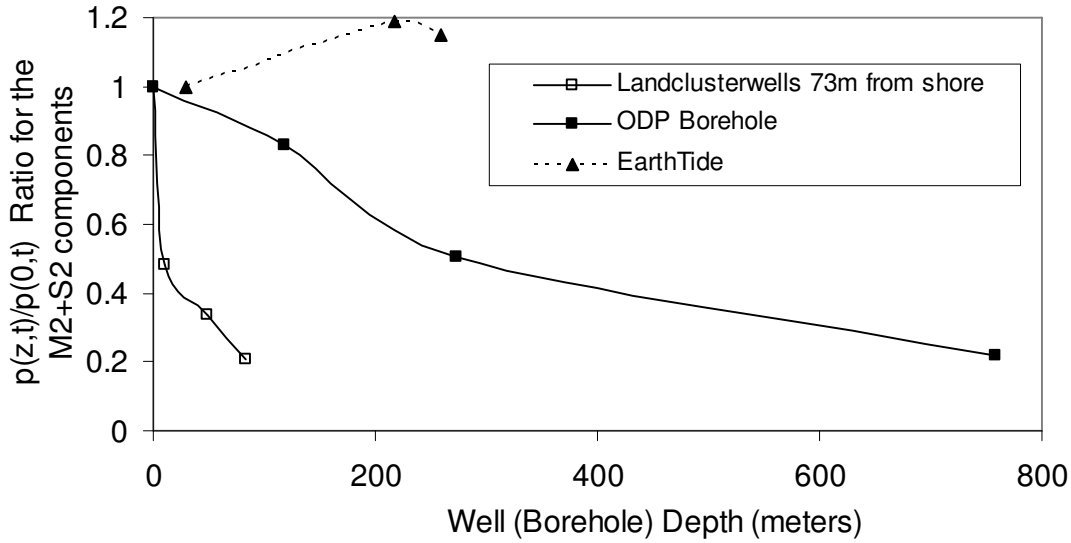

Figure 11. The p(z,t)/p(0,t) ratios of semi-durnal tide M2+S2 for clustered land wells near shore, ODP borehole and earthtide wells.

From equation (6), it is clear that as the depth z increases, the amplitude of diffusion for the ocean tidal loading decreases and approaches zero at infinity. Therefore, the ratio of the water level fluctuation at depth to the tidal water level fluctuation at sea/river floors, *p(z,t)/p(0,t)* will approaches the value of loading efficiency γ, i.e, $p(z,t)/p(0,t) \approx \gamma$ as indicated by Jupp (2000). According to Van Der Camp and Gale (1983), the loading efficiency γ ranges from 0.22 to 0.54 (approximately averaged 0.38). On average, that means one third of the ocean tidal loading signals may never damp. From Figure 11, the $p(z,t)/p(0,t) \approx \gamma$ of diurnal tidal components (M2+S2) vs. the depth plot, those oceanic tidal ratios damp exponentially with depth while the earth tidal amplitude increases with depth. The *p(z,t)/p(0,t)* of oceanic semidiurnal tide approximates to 0.2 for both the ODP hole 857D which was screened at a depth of 580 to 936 meters below seafloor and one of the deeper clustered land wells HADE181 which is screened at an average depth of 83 meters in Maryland (Figures 11 and 6). The ratios of *p(z,t)/p(0,t)* of oceanic diurnal tide (K1+O1) are approximately 0.19 in both locations. It seems that the ratios of *p(z,t)/p(0,t)*, i.e., the loading efficiency γ could decrease further below 0.2 as the well depth increases based on Figure 11. This indicates that the influence of the loading efficiency γ may be smaller than that of the theoretical prediction.

We apply the above solution (6) to pressure time series data of ODP hole 1025C for only the oceanic tidal loading (see Figure 4, for location). Because more than 29 days of fluid pressure data for this particular site was available, Boon and Kiley's (1978) harmonic analysis was applied to the filtered pressure time series. The depth of the open hole for hole1025C is about 100 meters below the seafloor based. Unconfined conditions are assumed for the rock/sediment layer. The 25 major tidal constituents extracted from the harmonic analysis (see Table 1 for the names of the constituents) are programmed into (4). The tidal speed is calculated by $a_k=2\pi/T_k$., where T_k. is the tidal period of the kth tidal constituent. The average porosity value of 60% for hole 1025C from ODP report (Shipboard Scientific Party, 1997) is used. Assuming a smaller loading efficiency $\gamma=0.1$, using a calibrated

specific storage/conductivity (S_s/K) ratio of 1.13×10^{-5} in Eq. (4), the multi-tidal constituent prediction is computed and drawn in Figure 12. It is apparent that the latter provides a fairly good fit with the measured data of ODP hole1025C.

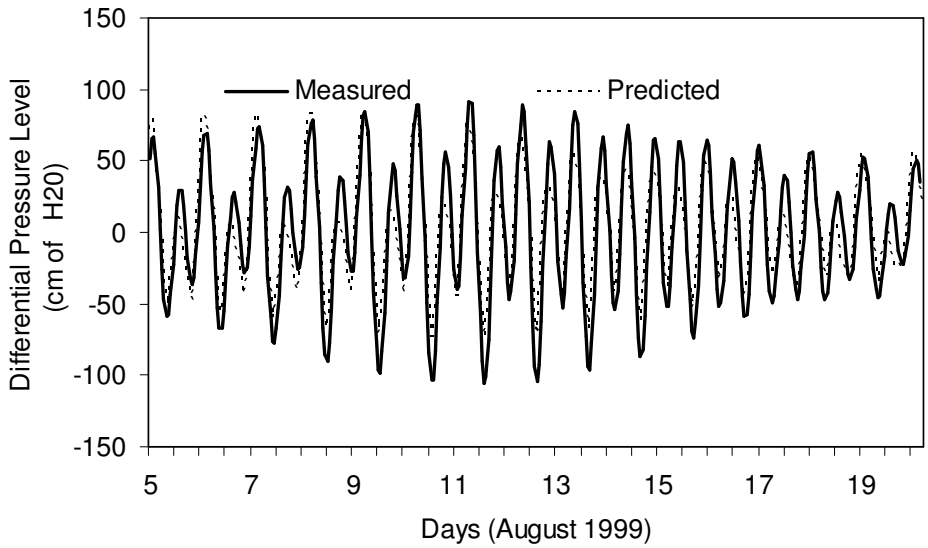

Figure 12. Comparison of measured water level vs. zero-order predicted water level time series for the ODP hole 1025C.

From the correlations between the tidal signals and the geothermal temperature fluctuations indicated in Section 2.3, one may be able to predict fluctuations of the temperature from variations of the borehole fluid pressure. It is likely that the observed thermal fluctuations in the borehole are the combination result of the flow and change of state of thermal fluid induced by tidal pressure fluctuations.

CONCLUSIONS

We have summarized and verified in this paper through numerous approaches that tides can trigger a whole manifold of complicated geological phenomena. Tidal effects on ground water pressures are now well recognized and may be used to infer important hydraulic properties of aquifers. Results of numerous ODP projects in recent years have also indicated tidal effects on geothermal temperature fluctuations and on microseismicity at mid-oceanic ridge systems. Our data analysis provides further evidence that, whereas tidal signals from the ocean load propagate deep into the sediments, with their tidal amplitudes decreasing with depth, signals from the earth (body) tide increase with depth, if one assumes that the porosity of the aquifer system decreases with depth. The vertically damped tidal influence in a coastal aquifer means that prediction of water level fluctuations in a monitoring well will need to consider the screen depth of the well. For an ODP mid-oceanic ridge borehole we have shown that, the periodical temperature variations in response to the tidal loading may come mainly from the fluid dynamics or the loosely named “tidal pumping of fluids “ rather than the state of the thermal fluid change. The analytical discussion in the paper also shows that one can predict the

vertical pressure changes both in a land well and ODP borehole.

ACKNOWLEDGEMENTS

The authors thank David Drummond of Maryland Geological Survey for providing the tidal level data in Bush River and Richard Saffer of USGS for providing the two water well data series. We are grateful to Earl Davis of Geological Survey of Canada for providing the details related to the ODP data we used in the paper.

REFERENCES

Anderson, G., Constable, S., Staudigel, H., Wyatt, F., K. (1997). A seafloor long-baseline tiltmeter. *Journal of Geophysical Research*, vol. 102, no.B9, p.20,269-20,285.

Bear, J., (1972). *Dynamics of Fluids in Porous Media*. Dover Publications, Inc. New York.

Boon, J.D., Kiley, K.P.(1978). *Harmonic analysis and tidal prediction by the method of least squares,* Special Report No.186. Virginia Institute of Marine Science, Glocester Point, Birginia.

Bredehoeft, J.D.(1967). Response of Well-Aquifer Systems to Earth Tides, *Journal of Geophysical Research,* v. 72, no. 12, p. 3075-3087**.**

Callen, H.B. (1962). *Thermodynamics*. John Wiley and Sons, Inc., New York.

Carr, P. A. and Van Der Kamp, G. S. (1969). Determining aquifer characteristics by tidal method, *Water Resour. Res.,* 5, 1023-1031.

Carslaw, H. S. and Jaeger, J.C. (1959), *Conduction of Heat in Solids*. Oxford at the Clarendon Press.

Cox, R.A. and Smith, N.D.(1959). The specific heat of sea water. Proc. Roy. Soc. London, Ser., A., 252, 51-62.

Davis, E.E. and Becker, K.(1994). Formation temperatures and pressures in a sedimented rift hydrothermal system: 10 months of Cork observations, Holes 857D and 858G. *Proceedings of the Ocean Drilling Program*, Scientific Results, vol., 139, p.649-666.

Davis, E. E., and Becker, K.(1999). Tidal pumping of fluids within and from the oceanic crust: new observations and opportunities for sampling the crustal hydrosphere. *Earth and Planetary Science Letters*, Vol., 172, pp.141-149.

Davis, E.E., Becker, K., Wang, K. and Carson, B. (995). Long term observations of pressure and temperature in hole 892B, Cascadia accretionary prism. *Proceedings of the Ocean Drilling Program, Scientific Results*, vol., 146, p.299-311.

Davis, E.E., Wang,K., Becker, K. and Thomson, R.E.(2000). Formation scale hydraulic and mechanical properties of oceanic crust inferred from pore pressure response to periodic seafloor loading. *Journal of Geophysical Research*, vol.,105, p.13,423-13,435.

Davis, E.E., Wang, K., Thomson, R.E., Becker, K., Cassidy, J.F. (2001). An episode of seafloor spreading and associated plate deformation inferred from crustal fluid pressure transients., *Journal of Geophysical Research*, vol.,106, no.B10, p.21,953-21,963.

Drummond, D.D. and Blomquist,J.D.(1993). *Hydrogeology, Water Supply Potential, and Water*

quality of the coastal plain aquifers of Harford County, Maryland. Report of Investigation No.58, Maryland Geological Survey.

Feistel, R. (2003).A new extended Gibbs thermodynamic potential of seawater, Progress in Oceanography 58, 43–114

Foreman, M. G.G. (1979). *Manual for tidal heights analysis and prediction*, Institute of Ocean Sciences, Patricia Bay, Victoria, B.C.

Fufonoff, N.P. (1985). Physical properties of sea water: A new salinity scale and equation of state for sea water. *Journal of Geophysical Research*, vol.,90, No. C2, pp. 3332-3342.

Fujioka, K., Kobayashi, K., Kato, K., Aoki, M., Mitsuzawa, K., Kinoshita, M. & Nishizawa, A. (1997), Tide-related variability of TAG hydrothermal activity observed by deep-sea monitoring system and OBSH, Earth and Planetary Science Letters, Vol. 153, pp. 239 – 250.

Hsieh, P., Bredehoeft, J. and Far, J.M.(1987). Determination of aquifer transmissivity from earth tide *analysis. Water Resources Research*, vol, 23,no.10, p.1824-1832.

Johnson, H.P., and Tunnicliffe, V.(1985). Time-series measurements of hydrothermal activity on northern Juan de Fuca Ridge. *Geophysical Research Letters*, Vol.,12, No.10, pp.685-688.

Jupp, T.E. (2000). *Fluid flow processes at Mid-Ocean ridge hydrothermal systems*. PhD dissertation, Pembroke College, University of Cambridge.

Kinoshita, M., Von Herzen, P.R., Matsubayashi, O., and Fujioka, K. (1998). Erratum to "Tidally-driven effluent detected by long-term temperature monitoring at the TAG hydrothermal mound, Mid-Atlantic Ridge', *Physics of the Earth and Planetary Interiors*, Vol., 109, pp.201-212.

Kovac, G. (1981). Seepage Hydraulics. 730 pp. Elsevier Science, New York.

Little, S.A., Stolzenback, K.D. and Grassle, F.J. (1988). Tidal currents effects on temperature in diffuse hydrothermal flow: Guaymas Basin, *Geophysical Research Letters*, Vol. 16, No.8, pp.985-986.

Marine, W. (1975). Water level fluctuation due to earth tides in a well pumping from slightly fractured crystalline rock. Water Resources Research, Vol, 11., no.1, p.165-173.

Melchior, P. (1983). The Tides of the Planet Earth, Pergamon, New York.

Millero, F. J., Chen, C. -T., Bradshaw, A., & Schleicher, K. (1981). Summary of data treatment for the international high pressure equation of state for seawater. Unesco technical papers in marine science, 38, 99–192.

Millero, F.J., Perron G.and Desnoyers, J.E. (1973). Heat capacity of seawater solutions from 5 to 35 ^{o}C and 0.5 to 22 ‰ chlorinity. Journal of Geophysical Research, vol.78, no.21, p. 4499-4507.

Rojstaczer, S. and Agnew, D.C. (1989). The influence of formation material properties on the response of water levels in wells to earth tides and atmospheric loading, *Journal of Geophysical Research,* Vol. 94, pp. 12403 – 12411.

Rojstaczer, S. And Riley, F.S. (1990). Response of the water level in a well to earth tides and atmospheric loading under unconfined conditions. *Water Resources Research*, Vol. 26, no.28, p.1803-1817.

Rydelek, P.A., Davis, P.M. and Koyanagi, R.Y. (1988). Tidal triggering of earthquake swarms at Kilauea volcano, Hawaii. *Journal of Geophysical Research*, vol., 93, no.B5, p.4401-4411.

Schultz, A., Delaney, J.R. and McDuff, R.E. (1992). On the partitioning of heat flux between diffuse and point source seafloor venting. *Journal of Geophysical Research*, Vol.97, No.B9, pp.12,299-12,314.

Shipboard Scientific Party, (1997). *Proceedings of the Ocean Drilling Program, Initial Report*, Vol. 168.

Sun, H.(1997). A two-dimensional analytical solution of groundwater response to tidal loading in an estuary. *Water Resources Research*. Vol.33, No.6, p.1429-1435.

Sun, H. and Koch, M. (1998). Cyclic movement of water particles in a coastal aquifer due to tidal loading. In *Environmental Coastal Regions*, edited by C.A. Brebbia, p.403-414. Computational Mechanics Publications, WITpress, Boston.

Sun, H. and Koch, M.(1999). Tidal and non-tidal characteristics of flow and water levels in Apalachicola Bay, Florida. In *Coastal Engineering and Marina Development*, (edited by Brebbia and Anagnostopoulos), p. 357-366. WIT press, Southampton, Boston.

Thurman, H.V., and Trujillio (1999). Essentials of Oceanography, Prentice Hall.

Tolstoy, M., Vermon, F.L., Orcutt, J,A., Wyatt, F.K., (2002), Breathing of the seafloor: Tidal correlations of sismicity at Axial volcano., *Geology*, vol.30, no.6, p.503-506.

Van Der Kamp, G. and Gale, J.E. (1983). Theory of earth tide and barometric effects in porous formation with compressible grains. *Water Resources Research*, vol., 19, no.2, p.538-544.

Wagner W. and Pruβ, A. (2002), The IAPWs formulation 1995 for the thermodynamic properties of ordinary water substance for general and scientific use. *Journal of Physical and Chemical Reference Data*, Vol., 31, No.2. p.387-535.

Wang, J. and Davis, E., E. (1996). Theory for the propagation of tidally induced pore pressure variations in layered subseafloor formations. *Journal of Geophysical Research*, vol. 101, no.B5, p.11,483-11,495.

Wang, K., Van der Gamp, G., Davis, E.E. (1999). Limits of tidal energy dissipation by fluid flow in subsea formations. *Geophysical Journal International*, v. 139, p.763-768.

Wetzler, M.A., Lavell, J.W., Cannon, G.A., and Baker, E.T. (1998). Variability of temperature and currents measured near Pipe Organ hydrothermal vent site, *Marine Geophysical Research*, Vol., 20, No.6, pp.505-516.

Wilcock,W.S.D. (2001). Tidal triggering of microearthquakes on the Juan de Fuca Ridge. *Geophyscial Research Letters*, vol., 28, no.20, p.3999-4002.

Zaske, J., Zürn W., and Wilhelm, H. (2000). NDFW analysis of borehole water level data from the hot-dry-rock test Soultz-sous-Forets, *Bulletin d'Information des Marées Terrestres*, p.10241-10270.